Journal of Cluster Science (2023) 34:3001–3011
https://doi.org/10.1007/s10876-023-02430-x

ORIGINAL PAPER

A Systematic Study of Nanoliposomes Loaded with α-Al_2O_3 Quantum Dots Nanoparticles (QDNPs), in vivo Imaging Study

Aida Bahadori[1] · Negar Dehghan Noudeh[2] · Abbas Pardakhty[3] · Peyman Rajaei[4] · Mehdi Ranjbar[3]

Received: 4 October 2022 / Accepted: 17 March 2023 / Published online: 3 May 2023

Abstract

Nanoliposomes with a great surface area within nano scales of about 20–100 nm have acceptable stability profiles for direct drug carriers. The present study focuses on the nanoliposomes loaded with α-Al_2O_3 quantum dots nanoparticles (QDNPs) for the in vivo imaging study. The final nanoliposomes loaded with α-Al_2O_3 QDNPs were synthesized with the microwave irradiation method and characterized with scanning electron microscopy (SEM), Fourier transformed infrared spectrum (FT-IR), thermo-gravimetric analysis (TGA), the average particle size can estimate between about 11 and 20 with transmission electron microscopy (TEM) and dynamic light scattering (DLS). The optical properties were evaluated with Uv-vis spectroscopy, and injected 0.001 mg/mL nanoliposomes loaded with α-Al_2O_3 NPs to the right leg (Balb/c male). The synthesis parameters such as power, irradiation time and concentration were designed by 2 k factorial. According to the analysis of variance experiments, it was found that the size of the minimum nanoparticles in this study was achieved at the highest irradiation time (15 min) and the lowest microwave power (180 watts) and α-Al_2O_3 concentration (0.05 g).

Keywords Quantum dots nanoparticles · In vivo imaging · Photoluminescence study · Nanostructures

Introduction

Nanoliposomes are a smaller variant of liposomes, one of the most widely used encapsulation and controlled release systems [1–4]. To gain a better understanding of nanoliposomes, we must first comprehend the earlier technology that they are based on namely, liposomes [5–7]. Liposome is derived from two greek words, lipos (fat) and soma (body or structure) and refers to a structure in which an aqueous compartment is encased by a fatty envelope [8, 9]. A liposomes (sometimes called bilayer lipid vesicles) are excellent cell and biomembrane models [10, 11]. Because of their likeness to biological membranes [12], they are a perfect system for studying not only modern biomembranes [13, 14] but also the emergence, function and evolution of primitive cell membranes [15, 16]. These structures are also employed as carrier systems by the food, cosmetics, agricultural [17, 18] and pharmaceutical industries [19] for the protection [20] and transportation of various materials like medicines [21], nutraceuticals [22], insecticides [23] and genetic material [24, 25]. Liposomes are made up of one or more concentric or nonconcentric lipid and phospholipid bilayers and biodegradable substrates for biomarkers and in drug delivery [26–28], and they can also contain other molecules like proteins [29, 30]. They can be single or multilamellar in terms of the number of bilayers they contain [31], and their aqueous and/or lipid compartments can accept hydrophilic, lipophilic [32] and amphiphilic molecules[33]. Liposomes and nanoliposomes have similar chemical, structural and thermodynamic features in general; these structures with quantum dots can increase the speed of cell penetration and intratissue process with high efficiency [34]. Nanoliposomes, on the other hand, have a larger surface area than liposomes and hence have the potential to increase solubility [35], improve bioavailability [36], improve controlled release [37] and enable more precise targeting of the encapsulated material

✉ Mehdi Ranjbar
Mehdi.Ranjbar@kmu.ac.ir

1 Student Research Committee, Kerman University of Medical Sciences, Kerman, Iran

2 Cumming School of Medicine, University of Calgary, 3330 Hospital Dr NW, Calgary, AB T2N 4N1, Canada

3 Pharmaceutics Research Center, Institute of Neuropharmacology, Kerman University of Medical Sciences, Kerman, Iran

4 Department of Biology, Kerman Branch, Islamic Azad University, Kerman, Iran

[38]. Quantum dots (QDs), as a group of semiconducting nanomaterials, have advantages for wide applications in biology, they are used as markers for specific cells such as luminescent probes [39], labeled cancer cells [40] and transplanted cells from host cells [41]. Nanoliposomes, also known as submicron bilayer lipid vesicles are a relatively new technology for encapsulating and delivering bioactive substances the use of QD luminescent labels has the potential to eliminate most of these problems [42]. Nanoliposomes have potential uses in a wide range of disciplines, including nanotherapy (e.g. diagnosis, cancer therapy, gene transfer), cosmetics [43], food technology [44], and agriculture [45], due to their biocompatibility and biodegradability [46], as well as their nanosize. QDs as semiconductor nanoparticles (e.g. CdSe, InP, InAs) with diameters in the range of 2 to 10 nm are spherical nanoparticles with a diameter of a few nanometers that are highly emissive [47]. They serve as a platform for a family of materials that can be used in light emitting diodes, photovoltaic cells, and biosensors. The synthesis of quantum dots has gotten a lot of interest in recent years because of its unique optical, chemical, and electrical features which can decrease the systemic side effects of anticancer drugs through effectively increasing the surface-to-volume ratio [10, 48]. Fluorescence labeling as a safe and high efficiency method used for tracing and measuring nanoliposomes in vivo study [49]. Liposomes have shown advantages as drug carriers but they are associated with problems related to physical stability such as aggregation, sedimentation and leakage on storage. In this study, by preparing nanoliposomes loaded with α-Al_2O_3 nanoparticles, in addition to increasing the stability of the liposomes unique optical properties for use in smart drug delivery and targeted treatment of cancer cells was inducing in these structures.

In this study nanoliposomes bilayer lipid vesicle as a new structure for the encapsulation and delivery of α-Al_2O_3 quantum dots agents for in vivo imaging study. The final nanoliposomes loaded with α-Al_2O_3 quantum dots nanoparticles were characterized with DLS, SEM, TEM, TGA, FT-IR and Uv-vis spectroscopy.

Experimental

Methods and Materials

All of the materials required to carry out this research project were without further purification. The crystallinity structure of Al_2O_3 quantum dots nanoparticles (QDNPs) investigated using of X-Ray Diffraction with specifications a Rigaku D-max C III, X-ray diffractometer using Ni-filtered Cu Ka radiation. Cholesterol and non-ionic surfactants (Span40, sorbitan monopalmitate ≤ 99.0%) were purchased from SRL Co, Italy. $Al(NO_3)_3.9H_2O$ (CAS No.7784-27-2, MW: 375.13 g/mol) and NaOH (Molar mass: 39.997 g/mol, ≤ 99.0%) were purchased from Merck company. Morphological properties evaluated with scanning electron microscopy (SEM), Philips XL-30 ESEM, and the transmission electron microscope (TEM, JEM1200EX, JEOL). The Fourier-transform infrared spectroscopy (FT-IR) spectra evaluated with Shimadzu Varian 4300 spectrophotometer in KBr pellets in the range of 500–3500 cm^{-1}. The size distribution estimated with Dynamic Light Scattering (DLS/measurement range 0.3 nm–10.0 microns/Malvern Panalytical GmbH—Herrenberg, Germany). UV-Vis diffuse reflectance spectroscopy analysis was carried out using Shimadzu UV-2600 spectrophotometer. Analysis of variance (ANOVA) was carried out using Design Expert 7.0.0 package (Stat-Ease, Inc., Minneapolis, MN, USA). For in vivo imaging study of QDNPs, the mice (Balb/c male Inbred rats purchased from Animal care center aged between 8 and 6 weeks) were feeded and raised according to the Institutional an Animal Care and Use Committee (IACUC) protocol. To investigate the optical properties in the living organism we injected 0.001 mg/mL nanoliposomes loaded with α-Al_2O_3 NPs to the right leg (Balb/c male).

Preparation of Nanoliposomes

For the preparation of the liposomal system, according to laboratory conditions, the method of watering a thin layer was selected [50]. In the first, 300 µL of surfactant (Span 40) and 76 µL Cholesterol was dissolved in 20 mL chloroform in a 150 mL round-bottomed flask in reflux system. Above solution was heated and stirred in a magnetic stirrer at 400 rpm and 45 °C for 2 h.

Then the material, under static conditions for 60–50 min, were deposited as thin solid layers in the bottom of the balloon. For hydration, dry the layer of PBS saline solution (saline buffered Phosphate) was used. For better hydration, thin solid layers in the bottom of the balloon were exposed under a hairdryer at 45 °C for 60 min. In the final the milky solution was placed in the sonicator bath for 45 min at 60 watts. The nanoliposomes were collected in a falcon tube for characterization and the next step.

Nanoliposomes Loaded with α-Al_2O_3 NPs

At the first, 0.05 g of $Al(NO_3)_3.9H_2O$ in 10 mL propylene glycol was added. Then 3 mL NaOH 2 M was added drop by drop to the above solution under 400 rpm for 30 min to get a homogeneous mixture. For the preparation of nanoliposomes loaded with α-Al_2O_3 NPs, 2 mL of the white α-Al_2O_3 solution was added to 5 mL of nanoliposomes put into Teflon, and reaction was performed under microwave irradiation system at the various power and time. In this

study, in order to design experiments, microwave irradiation and power were considered as variables and size were analyzed as a response.

Results and Discussion

Characterization

The results obtained from scanning electron microscopy (SEM) analysis show that the nanoliposomes based on lipid bilayers have been created as a carrier with suitable capacity for α-Al_2O_3 NPs. Figure 1A shows SEM images of the as synthesized nanoliposomes loaded with α-Al_2O_3 NPs in different concentrations such as 0.01 mg/mL (1a), 0.1 mg/mL (1b), 0.05 mg/mL (1c), 0.5 mg/mL (1d), 0.09 mg/mL (1e) and 0.9 mg/mL (1f) respectively. The new contract from as synthesized the α-Al_2O_3 NPs indicated a uniform substrate with the ability of connect to the nanoliposomes [51]. The relationship between concentrations of the α-Al_2O_3 NPs and the shape of the final formulation shows as the concentration of the α-Al_2O_3 NPs in the nanoliposomes as carriers, increases the adhesion of the structure increases significantly. This adhesion in the final formulation can be due to the increase in the surface-to-volume ratio of nanoparticles. The presence of porous holes in quantum dots is evident due to electron transfer cavity electron transfermate [52]. The PSA diagram of α-Al_2O_3 NPs is shown in Fig. 1B

To show the internal image of the nanoliposomes loaded with α-Al_2O_3 NPs we used transmission electron microscopy (TEM) analysis. The TEM image of the nanoliposomes loaded with α-Al_2O_3 NPs is shown in Fig. 2a. As the results show, two components including enclosed space and trapped nanoparticles can be easily detected. The core zone related to nanoliposomes which are dark borderline, is clearly visible. The α-Al_2O_3 NPs trapped in nanoliposomes as separate points are visible and the average particle size is estimated between 95 and 120. Figure 2b confirms the α-Al_2O_3 NPs particle size according to dynamic light scattering (DLS) analysis. The results show that the distribution number (Dn) in 10%: 11.17 nm, Dn 50%: 14.75 nm and Dn 90%: 20.38 nm. The particle size curve has a uniform distribution. The diffusion coefficient for the calculation of particle size distribution is obtained from the below relation:

$$\Gamma = D_t q^2 \tag{1}$$

where q is the scattering vector, given by $q = (4\pi n/\lambda).\sin(\theta/2)$. The refractive index of the solution is n. The wavelength of the laser light is λ, and the scattering angle is introduced with θ. Inserting D_t into the *Stokes–Einstein* equation according to Eq. 2 [53], solving for particle size is the final step.

$$D_h = k_B T / 3\Pi\eta D t \tag{2}$$

D_h, Dt *are* the hydrodynamic diameter and the translational diffusion coefficient. Also k_B, T and η are *Boltzmann's* constant, thermodynamic temperature and dynamic viscosity respectively.

In Fig. 3a, the Fourier transform infrared spectroscopy (FT-IR) is used for the investigation of the functional groups. The nanoliposomes as synthesized show the principal bands at about 2985 cm^{-1} and 2924 cm^{-1} which can be related to CH_2 stretching groups in the span and cholesterol chains.

In addition, the absorption band centered at 1741 cm^{-1} is assigned to C = O stretching in the nanoliposomes loaded with α-Al_2O_3 NPs. The band centered at 1631 cm^{-1} correspond to symmetric vibrations CH_2 groups in the final products. The band at about 1420 cm^{-1} is related to C–O–C groups in nanoliposomes. The band at about 1649 cm^{-1} and 950 cm^{-1} correspond with Al-O vibration in α-Al_2O_3 NPs. Connection points α-Al_2O_3 quantum dots nanoparticles to liposome structures occur through C-H bands. This can lead to the fabrication a new type of QDs with liposomes.

In this study thermos gravimetric analysis (TGA) technique used for physical and chemical characterization [54]. The first weight loss until about 130 °C is related to loss of adsorbed water from nanoliposomes loaded with α-Al_2O_3 NPs. The second mass loss can be related to the decomposition of the final products which happens in the range of 130 °C up to 150 °C which confirms that carbon chains between structures are broken. In this range carbon chains are broken in nanoliposomes as a carrier. After 150 °C up to 300 °C structural network at α-Al_2O_3 NPs is completely separated from each other and thermal degradation occurs. The differential thermal analysis (DTA) shows two endothermic transformations. The first strong peak occurs in the range of 130 °C up to 150 °C which can be related to phase transitions and the second occurs between 230 °C up to 240 °C due to melting points. TGA/DTA curves of nanoliposomes loaded with α-Al_2O_3 NPs are shown in Fig. 3b.

Statistical Analyses

According to the analysis of variance (ANOVA) experiments were performed regarding one replicate and three center points (2^{3-1}). The effects of the independent variables on the experimental design and obtained the final equation in terms of coded factors are represented in Table 1.

The mathematical relationship between the three factors was estimated by the two-factor interaction model equation.

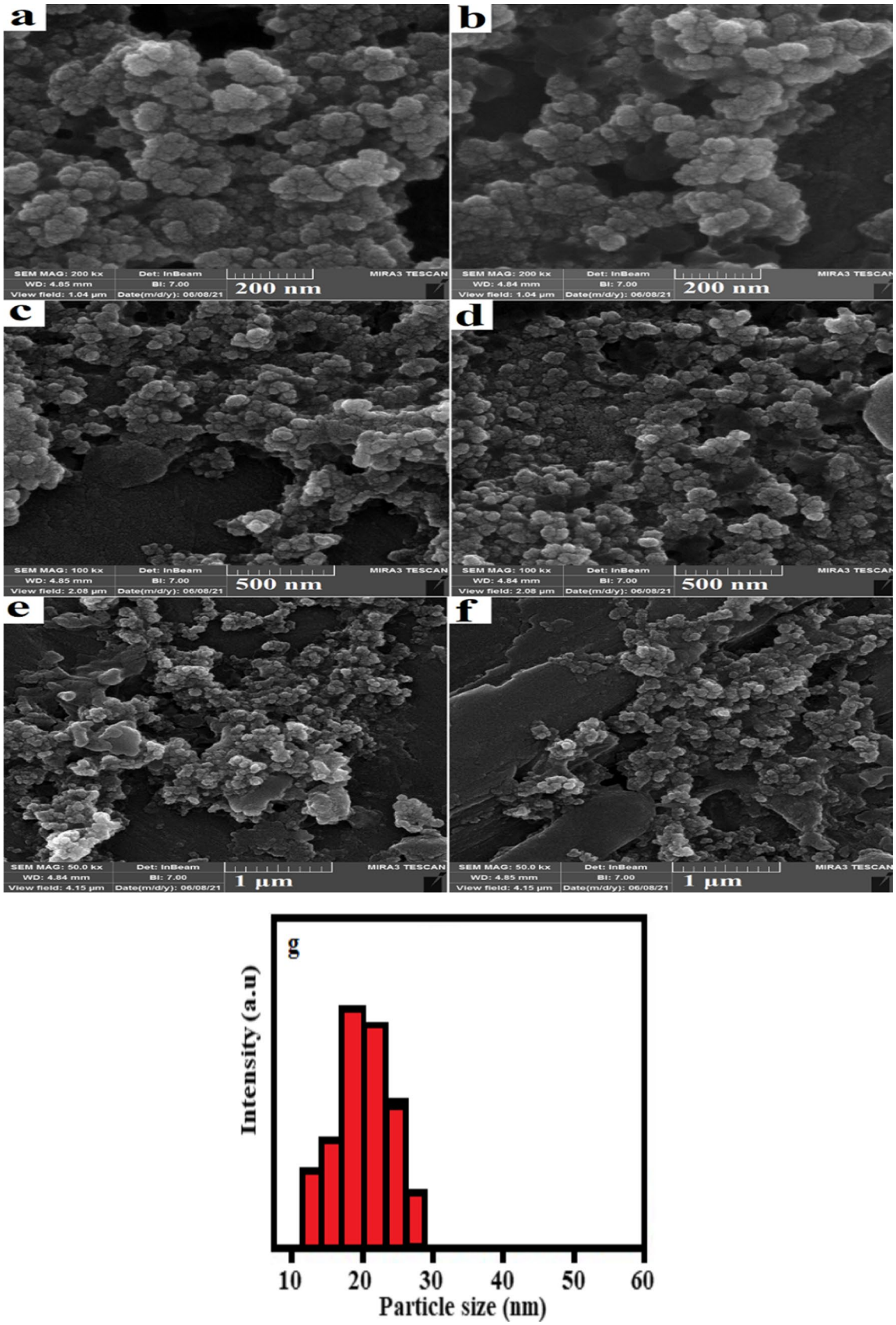

Fig. 1 **A** SEM images of the as synthesized nanoliposomes loaded with α-Al_2O_3 NPs in different concentrations such as 0.01 mg/mL (a), 0.1 mg/mL (b), 0.05 mg/mL (c), 0.5 mg/mL 1d, 0.09 mg/mL 1e and 0.9 mg/mL 1f respectively. The PSA diagram of α-Al_2O_3 NPs (**B**)

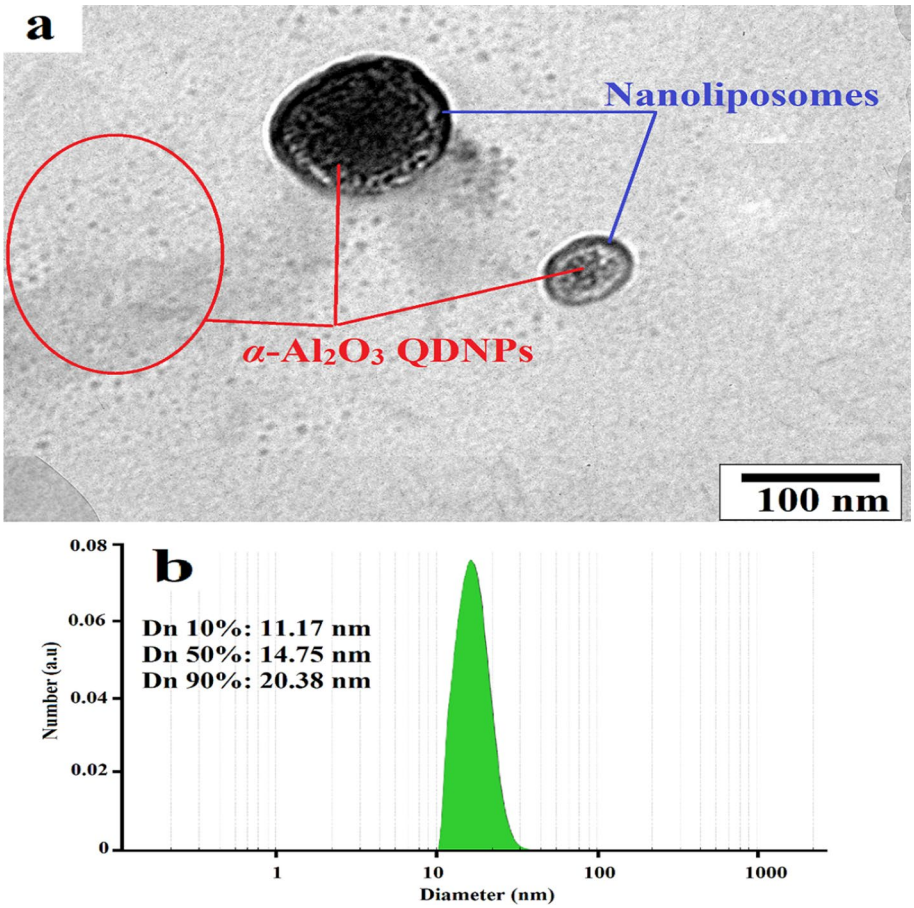

Fig. 2 **a** The TEM image of the nanoliposomes loaded with α-Al_2O_3 NPs (**a**) and DLS diagram of α-Al_2O_3 NPs

$$R = +17.25 + 4.25\ A - 3.75\ B + 4.25\ BC + 2.75\ ABC \quad (3)$$

R is the predicted response (size), A, B and C represent the coded levels of the independent variables such as power, time and concentration in the statistical model. According to the ANOVA results, the model of the proposed study was significant ($p \leq 0.0001$) while the lack of fit of the model was not significant ($p \geq 0.9502$). The difference between Adj R-squared (0.7627) and pred R-squared (0.7601) is estimated at about 0.0026, which shows that the model argument is very accurate.

Figure 4a, b and c show three-dimensional (3D) contour plots, the effects of the α-Al_2O_3 quantum dots nanoparticles concentration, irradiation time and microwave power on the final size of nanoliposomes loaded with α-Al_2O_3 quantum dots nanoparticles. The minimum nanoparticles size in this study was achieved at the highest irradiation time (15 min) and the lowest microwave power (180 watts) and α-Al_2O_3 concentration (0.05 g).

Therefore, according to the suggested model, the Pred R^2 is in reasonable agreement with the Adj R^2 which shows that there is an excellent correlation between the predicted values and the experimental results ($R^2 = 0.9941$). Figure 5a and b show desirability and predicted vs. actual in statistical analyses. The results show that the effect of the variables irradiation time and microwave power on the particle size response of the final products are very significant compared to α-Al_2O_3 concentration. According to the model calculations, the best size (8.41 nm) with the highest desirability can be obtained at microwave power (180.29 watts), irradiation time (14.99 min) and α-Al_2O_3 concentration (0.06 g).

Table 2 shows that the model of the study is significant, while the lack of fit of the model was not significant ($p \geq 0.9502$). The Model F-value of 8.23 implies the model is significant. There is only a 2.00% chance that a "Model F-Value" this large could occur due to noise. The "Curvature F-value" of 22.70 implies there is significant curvature (as measured by the difference between the average of the center points and the average of the factorial points) in the design space. There is only a 0.50% chance that a "Curvature F-value" this large could occur due to noise.

Optical Properties and in vivo Study

For the investigation of the optical properties of nanoliposomes loaded with α-Al_2O_3 NPs we used UV-Vis absorption spectroscopy in room temperature. In Fig. 6a, the absorption spectra show a strong peak in the wavenumber

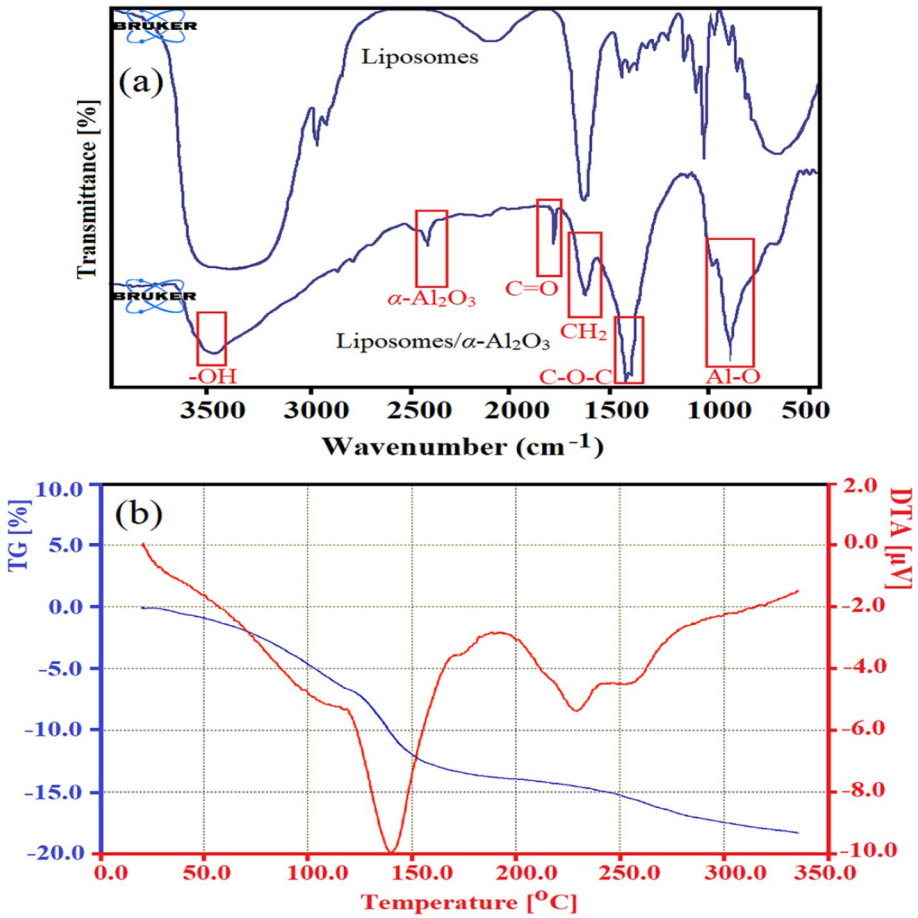

Fig. 3 The FT-IR spectrum (**a**) and TGA/DTA profile of the nanoliposomes loaded with α-Al_2O_3 NPs (**b**)

Table 1 Coefficient estimate and confidence limit low and high in the suggested model

Factor	Coefficient estimate	Degree of freedom	Standard error	95% confidence limit low	95% confidence limit high
Intercept	17.25	1	1.32	13.85	20.65
A-power	4.25	1	1.32	0.85	7.65
B-time	− 3.75	1	1.32	− 7.15	− 0.35
BC	4.25	1	1.32	0.85	7.65
ABC	2.75	1	1.32	− 0.65	6.15
Center point	12.08	1	2.54	5.56	18.60

of about 225 nm. This is blue shift relative to the empty liposomes as potential vehicles [55]. The UV-Vis absorption spectroscopy data shows well that the presence of α-Al_2O_3 NPs has created unique optical properties for in vivo imaging [56, 57]. The results show a good light reflection in nanoliposomes loaded with α-Al_2O_3 NPs compared to the blank sample and the liposomes sample only. The nanoliposomes loaded with α-Al_2O_3 NPs have been highly efficient in vivo research due to the distance between the conduction levels and capacitance levels through appropriate light emission [58]. To investigate the optical properties in the living organism we injected 0.001 mg/mL nanoliposomes loaded with α-Al_2O_3 NPs to the right leg (Balb/c male). Then a 1:2 ratios of ketamine/xylazine was injected for anesthesia immediately. After 3 min, the optical properties of nanoliposomes loaded with α-Al_2O_3 NPs is clearly visible on the right leg. How to inject into mice and in vivo image of mice after 3 min are illustrated in Fig. 6b and c respectively. The bright spots indicate α-Al_2O_3 quantum dots nanoparticles with high luminescence activity due to the quantum effect. The existence of the quantum dot structure gives a significant synergistic effect in image formation at in vivo imaging studies. The bright white spots are characteristic α-Al_2O_3 quantum dots nanoparticles and this can be due to the unique

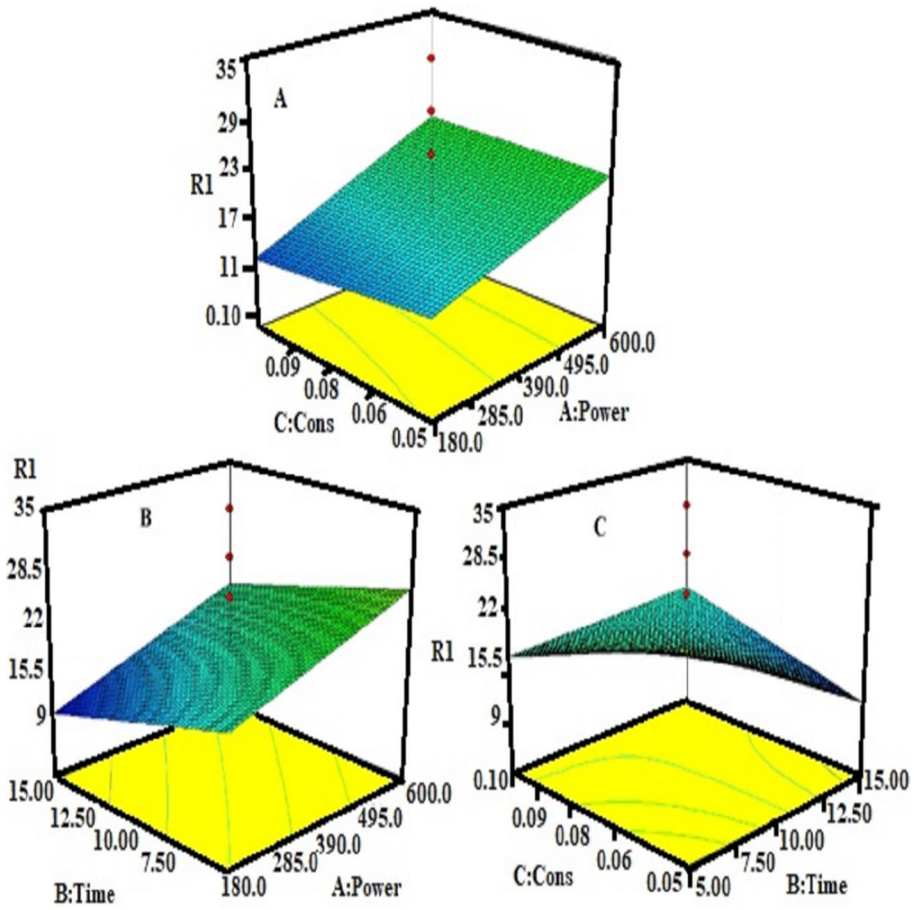

Fig. 4 Three-dimensional (3D) contour plots, the effects of Vconcentration (**A**), microwave power (**B**) and irradiation time (**C**) on the final size of nanoliposomes loaded with α-Al_2O_3 quantum dots nanoparticles

properties through a high surface-to-volume ratio from these structures. This shows that quantum dots nanoparticles absorb more amount drugs on their surface.

X-ray diffraction technique in room temperature of α-Al_2O_3 quantum dots nanoparticles is indicating in Fig. 7. The presence of peaks with the same position peaks of XRD patterns of Al_2O_3 nanoparticles show crystal phase have been formed. The X-ray diffraction measured in the range of $10 < 2\Theta < 80$. The X-ray diffraction analysis indexed as 27.1° and 38.8° could be have in positions as (121), (211). The crystallographic parameters for Al_2O_3 were a = 4.7606 A°, b = 4.7606 A°, c = 12.9940 A° and crystal system was rhombohedral.

Conclusion

The nanoliposomes, as bilayer lipid vesicles, have the ability to encapsulate hydrophilic and hydrophobic drugs. In this study these nano-systems loaded with α-Al_2O_3 quantum dots nanoparticles as targeted tracking drug delivery carriers. According to the ANOVA results designed by 2 k factorial, the model was significant ($p \leq 0.0001$) and the minimum size for nanoliposomes loaded with α-Al_2O_3 quantum dots nanoparticles was achieved at the highest irradiation time (15 min), the lowest microwave power (180 W) and α-Al_2O_3 concentration (0.05 g). The final products were characterized with DLS, SEM, TEM, TGA, FT-IR and UV-vis spectroscopy. In vivo study results show nanoliposomes loaded with α-Al_2O_3 quantum dots nanoparticles have good potential for creating optical properties in targeted drug delivery carriers.

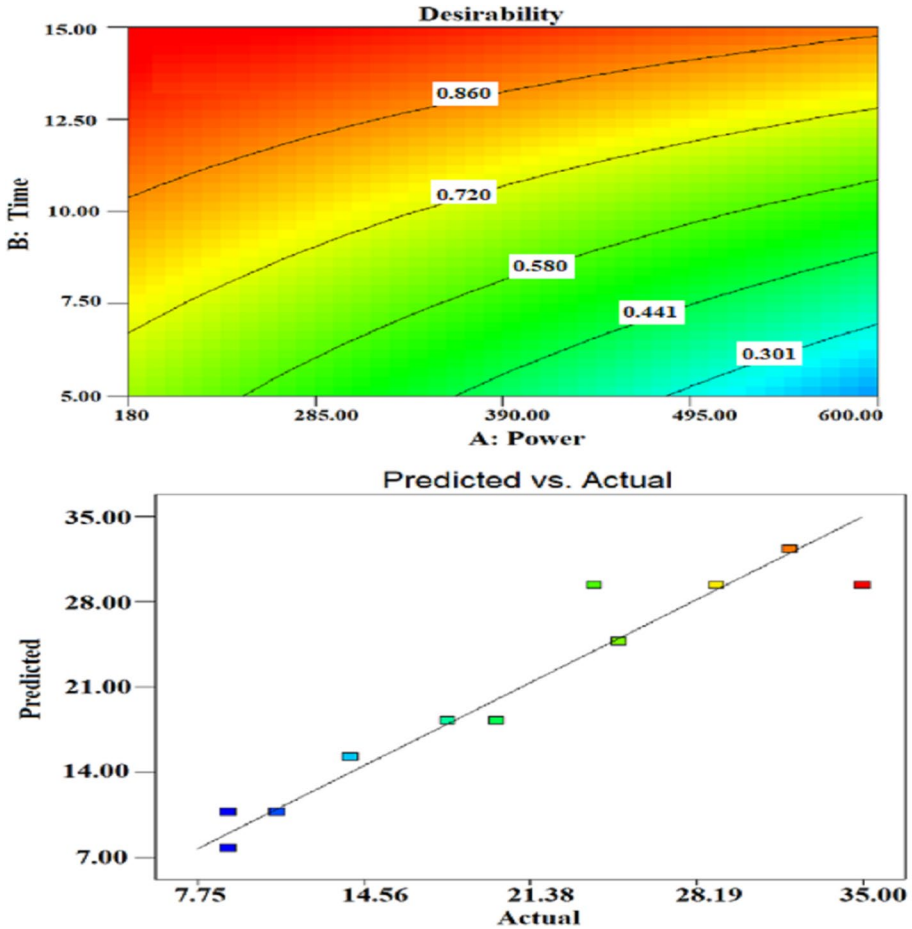

Fig. 5 Desirability diagram (**a**) and predicted vs. actual (**b**) in statistical analyses

Table 2 Analysis of variance (ANOVA) of medium components related to size response as per two-level factorial design

Source	Sum of squares	Degree of freedom	Mean square	F-value	P-value Prob > F
Model	462.00	4	115.50	8.23	0.0200
A-power	144.50	1	144.50	10.30	0.0238
B-time	112.50	1	112.50	8.02	0.0366
BC	144.50	1	144.50	10.30	0.0238
ABC	60.50	1	60.50	4.31	0.0925
Curvature	318.56	1	318.56	22.70	0.0050
Residual	70.17	5	14.03		
Lack of Fit	9.50	3	3.17	0.10	0.9502
Pure Error	60.67	2	30.33		

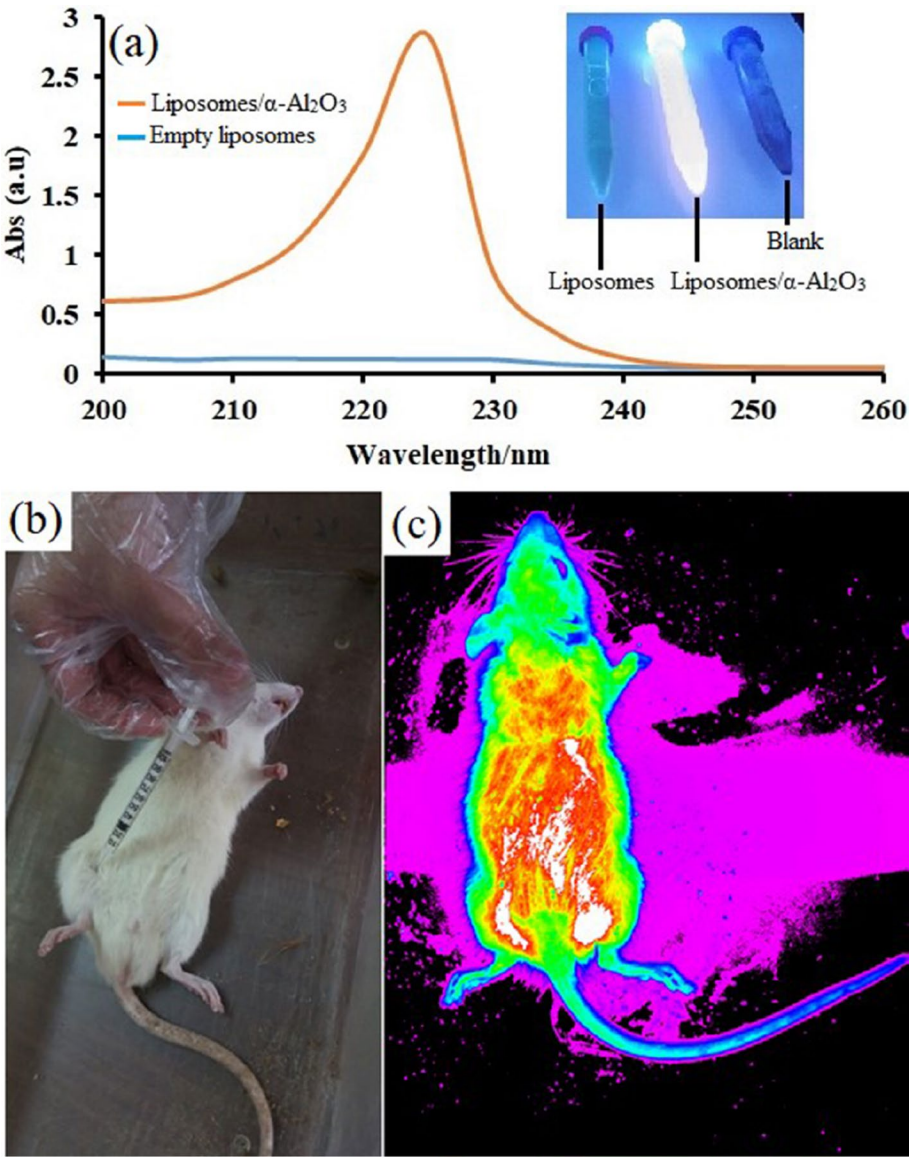

Fig. 6 The UV spectrum of the nanoliposomes loaded with α-Al_2O_3 quantum dots nanoparticles (**a**) and inject into mice (**b**) and in vivo image of mice 3 min after of injection (**c**)

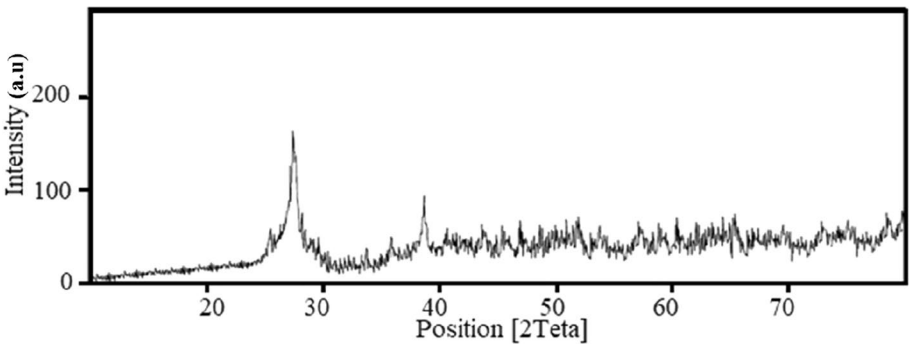

Fig. 7 X-ray diffraction patterns of α-Al_2O_3 quantum dots nanoparticles

Acknowledgements Institute of Neuropharmacology, Kerman University of Medical Sciences, also Laboratory of Nanostructures and Nanodrugs Materials, Kerman,Iran. This study received ethical approval (96000861) and (IR.KMU.REC.1396.2245) from the local ethical committee of the Kerman University of Medical Sciences.

Author Contributions NDN: developed the concept, edit text. AP: designed and carried out experimental work, analyzed the results, and prepared the manuscript, MR: designed and carried out experimental work, analyzed the results, and prepared the manuscript. PR: designed and carried out experimental work, analyzed the results, and prepared the manuscript.

Declarations

Competing interest The authors declare that no competing interests exist.

References

1. K. Uma Suganya, et al. (2017). Nanoscale chlorophyll-liposome composite (NCLC) fluorescent probe for in vivo bio-imaging. *J Clust Sci* **28** (5), 2969–2977.
2. Z. Fakhravar, et al. (2016). Nanoliposomes: synthesis methods and applications in cosmetics. *J Cosmet Laser Ther* **18** (3), 174–181.
3. I. Katouzian and S. M. Jafari (2016). Nano-encapsulation as a promising approach for targeted delivery and controlled release of vitamins. *Trends Food Sci Technol* **53**, 34–48.
4. S. Vahabi and A. Eatemadi (2017). Nanoliposome encapsulated anesthetics for local anesthesia application. *Biomed Pharmacother* **86**, 1–7.
5. X. Pang, et al. (2019). Bacteria-responsive nanoliposomes as smart sonotheranostics for multidrug resistant bacterial infections. *ACS Nano* **13** (2), 2427–2438.
6. M. Hasan, et al. (2019). Preparation, characterization, and release kinetics of chitosan-coated nanoliposomes encapsulating curcumin in simulated environments. *Molecules* **24** (10), 2023.
7. V. Karthick, et al. (2014). Effect of biologically synthesized gold nanoparticles on alloxan-induced diabetic rats—an in vivo approach. *Coll Surf Biointerf* **122**, 505–511.
8. M. Mozafari, Nanoliposomes: preparation and analysis,. Liposomes. Springer, pp 29–50.
9. B. Ding, et al. (2011). Preparation, characterization and the stability of ferrous glycinate nanoliposomes. *J Food Eng* **102** (2), 202–208.
10. C. Su, et al. (2018). Analytical methods for investigating in vivo fate of nanoliposomes: a review. *J Pharm Anal* **8** (4), 219–225.
11. L. Pan, H. Wang, and K. Gu (2018). Nanoliposomes as vehicles for astaxanthin: characterization, in vitro release evaluation and structure. *Molecules* **23** (11), 2822.
12. H. Watson (2015). Biological Membranes. *Essays Biochem* **59**, 43–69.
13. S. M. Santos, et al. (2014). Interaction of fullerene nanoparticles with biomembranes: from the partition in lipid membranes to effects on mitochondrial bioenergetics. *Toxicol Sci* **138** (1), 117–129.
14. N. T. Tran, F. Mentink-Vigier, and J. R. Long (2020). Dynamic nuclear polarization of biomembrane assemblies. *Biomolecules* **10** (9), 1246.
15. A. Pohorille and D. Deamer (2009). Self-assembly and function of primitive cell membranes. *Res Microbiol* **160** (7), 449–456.
16. S. Sarkar, et al. (2020). Prebiological membranes and their role in the emergence of early cellular life. *J Membr Biol* **253** (6), 589–608.
17. N. Morin-Crini, et al. (2019). Applications of chitosan in food, pharmaceuticals, medicine, cosmetics, agriculture, textiles, pulp and paper, biotechnology, and environmental chemistry. *Environ Chem Lett* **17** (4), 1667–1692.
18. R. Beck, S. Guterres, and A. Pohlmann, *Nanocosmetics and nanomedicines: new approaches for skin care* (Springer, 2011).
19. S. Anliker, et al. (2020). Quantification of active ingredient losses from formulating pharmaceutical industries and contribution to wastewater treatment plant emissions. *Environ Sci Technol* **54** (23), 15046–15056.
20. L. E. Escobar, A. Molina-Cruz, and C. Barillas-Mury (2020). BCG vaccine protection from severe coronavirus disease 2019 (COVID-19). *Proc Natl Acad Sci* **117** (30), 17720–17726.
21. F.-D. Cojocaru, et al. (2020). Nanomaterials designed for antiviral drug delivery transport across biological barriers. *Pharmaceutics* **12** (2), 171.
22. M. F. McCarty and J. J. DiNicolantonio (2020). Nutraceuticals have potential for boosting the type 1 interferon response to RNA viruses including influenza and coronavirus. *Prog Cardiovasc Dis* **63** (3), 383.
23. F. Matsumura, *Toxicology of insecticides* (Springer Science & Business Media, 2012).
24. A. K. Basak, et al. (2019). Silver nanoparticle–induced developmental inhibition of Drosophila melanogaster accompanies disruption of genetic material of larval neural stem cells and non-neuronal cells. *Environ Monitor Assess* **191** (8), 1–16.
25. D. Petrov, et al. (2019). Analysis of the effectiveness of the stages of the concentration of genetic material. *J Phys Conf Series.* **1400**, 033023.
26. Y. Peng, et al. (2018). Dual-targeting for brain-specific liposomes drug delivery system: synthesis and preliminary evaluation. *Bioorg Med Chem* **26** (16), 4677–4686.
27. D. Sharma, A. A. E. Ali, and L. R. Trivedi (2018). An updated review on: liposomes as drug delivery system. *PharmaTutor* **6** (2), 50–62.
28. M. Alavi, T. J. Webster, and L. Li (2022). Theranostic safe quantum dots for anticancer and bioimaging applications. *Micro Nano Bio Aspects* **1** (2), 1–11.
29. R. Esfandi, M. E. Walters, and A. Tsopmo (2019). Antioxidant properties and potential mechanisms of hydrolyzed proteins and peptides from cereals. *Heliyon* **5** (4), e01538.
30. J. A. Robinson (2019). Folded synthetic peptides and other molecules targeting outer membrane protein complexes in Gram-negative bacteria. *Front Chem* **7**, 45.
31. Y. Fan, et al. (2019). Multilamellar vaccine particle elicits potent immune activation with protein antigens and protects mice against Ebola virus infection. *ACS Nano* **13** (10), 11087–11096.
32. V. da Silva Santos, A. P. B. Ribeiro, and M. H. A. Santana (2019). Solid lipid nanoparticles as carriers for lipophilic compounds for applications in foods. *Food Res Int* **122**, 610–626.
33. W. Chu, et al. (2019). Low-toxicity amphiphilic molecules linked by an aromatic nucleus show broad-spectrum antibacterial activity and low drug resistance. *Chem Commun* **55** (30), 4307–4310.
34. Y. Cheng, et al. (2018). Cisplatin and curcumin co-loaded nanoliposomes for the treatment of hepatocellular carcinoma. *Int J Pharm* **545** (1–2), 261–273.
35. S. Amiri, et al. (2018). Vitamin E loaded nanoliposomes: effects of gammaoryzanol, polyethylene glycol and lauric acid on physicochemical properties. *Coll Interf Sci Commun* **26**, 1–6.
36. K. Suresh and A. Nangia (2018). Curcumin: pharmaceutical solids as a platform to improve solubility and bioavailability. *CrystEngComm* **20** (24), 3277–3296.
37. F. C. Kenechukwu, et al. (2018). Surface-modified mucoadhesive microgels as a controlled release system for miconazole nitrate to improve localized treatment of vulvovaginal candidiasis. *Euro J Pharm Sci* **111**, 358–375.
38. W. Jiang, et al. (2018). Cancer chemoradiotherapy duo: nano-enabled targeting of DNA lesion formation and DNA damage response. *ACS Appl Mater Interf* **10** (42), 35734–35744.

39. A. J. Sutherland (2002). Quantum dots as luminescent probes in biological systems. *Curr Opin Solid State Mater Sci* **6** (4), 365–370.
40. I. P. J. Lai, et al. (2016). Solid-state synthesis of self-functional carbon quantum dots for detection of bacteria and tumor cells. *Sens Actu Chem* **228**, 465–470.
41. A. Hoshino, et al. (2004). Applications of T-lymphoma labeled with fluorescent quantum dots to cell tracing markers in mouse body. *Biochem Biophys Res Commun* **314** (1), 46–53.
42. S. Akhavan, et al. (2018). Lipid nano scale cargos for the protection and delivery of food bioactive ingredients and nutraceuticals. *Trends Food Sci Technol* **74**, 132–146.
43. S.-B. Han, et al. (2021). Asterias pectinifera derived collagen peptide-encapsulating elastic nanoliposomes for the cosmetic application. *J Ind Eng Chem* **98**, 289–297.
44. M. R. Mozafari, et al. (2008). Encapsulation of food ingredients using nanoliposome technology. *Int J Food Prop* **11** (4), 833–844.
45. J. Wu, et al. (2015). The preparation, characterization, antimicrobial stability and in vitro release evaluation of fish gelatin films incorporated with cinnamon essential oil nanoliposomes. *Food Hydrocoll* **43**, 427–435.
46. M. Reza Mozafari, et al. (2008). Nanoliposomes and their applications in food nanotechnology. *J Liposome Res* **18** (4), 309–327.
47. H. F. Legg, et al. (2022). Giant magnetochiral anisotropy from quantum-confined surface states of topological insulator nanowires. *Nature Nanotechnol* **2022**, 1–5.
48. D. Huu Phuc, et al. (2021). The influence of dopant concentration on optical-electrical features of quantum dot-sensitized solar cell. *Molecules* **26** (10), 2865.
49. D.-E. Wang, et al. (2022). Colorimetric detection of alkaline phosphatase activity based on pyridoxal phosphate–induced chromatic switch of polydiacetylene nano-liposomes. *Microchim Acta* **189** (2), 1–12.
50. C. Tan, et al. (2013). Liposomes as vehicles for lutein: preparation, stability, liposomal membrane dynamics, and structure. *J Agric Food Chem* **61** (34), 8175–8184.
51. S. Mallakpour and F. Sirous (2015). Surface coating of α-Al2O3 nanoparticles with poly (vinyl alcohol) as biocompatible coupling agent for improving properties of bio-active poly (amide-imide) based nanocomposites having l-phenylalanine linkages. *Prog Org Coatings* **85**, 138–145.
52. X. Zhan, et al. (2022). Formation of multifaceted nano-groove structure on rutile TiO2 photoanode for efficient electron-hole separation and water splitting. *J Energy Chem* **65**, 19–25.
53. J. T. Edward (1970). Molecular volumes and the Stokes-Einstein equation. *J Chem Educ* **47** (4), 261.
54. T. Lécuyer, et al. (2022). Persistent luminescence nanoparticles functionalized by polymers bearing phosphonic acid anchors: synthesis, characterization, and in vivo behaviour. *Nanoscale* **14** (4), 1386–1394.
55. C. Chang, et al. (2021). Comparison of cubosomes and liposomes for the encapsulation and delivery of curcumin. *Soft Matter* **17** (12), 3306–3313.
56. W. Chen, et al. (2022). Near-infrared afterglow luminescence of chlorin nanoparticles for ultrasensitive in vivo imaging. *J Am Chem Soc* **144** (15), 6719–6726.
57. Y. M. Wang, et al. (2022). Single nano-sized metal–organic framework for bio-nanoarchitectonics with in vivo fluorescence imaging and chemo-Photodynamic therapy. *Nanomaterials* **12** (2), 287.
58. L. Zhao, et al. (2022). Direct investigations of the electrical conductivity of normal and cancer breast cells by conductive atomic force microscopy. *Ultramicroscopy* **237**, 113531.